Publication VI

Ala-Kleme, T., Mäkinen, P., Ylinen, T., Väre, L., Kulmala, S., Ihalainen, P., Peltonen, J., Rapid electrochemiluminoimmunoassay of human C-reactive protein at planar disposable oxide coated silicon electrodes, *Analytical Chemistry* **78** (2006) 82–88.

VI

Anal. Chem. **2006,** *78,* 82−88

Rapid Electrochemiluminoimmunoassay of Human C-Reactive Protein at Planar Disposable Oxide-Coated Silicon Electrodes

Timo Ala-Kleme,*,† Piia Mäkinen,† Tiina Ylinen,‡ Leif Väre,† Sakari Kulmala,‡ Petri Ihalainen,§ and Jouko Peltonen§

Department of Chemistry, University of Turku, FIN-20014 Turku, Finland, Laboratory of Inorganic and Analytical Chemistry, Helsinki University of Technology, P.O. Box 6100, FIN-02015 Hut, Helsinki, Finland, and Department of Physical Chemistry, Åbo Akademi University, Porthaninkatu 3, FIN-20500 Turku, Finland

Electrochemiluminescence (ECL) of aromatic Tb(III) chelates at thin insulating film-coated electrodes provides a means for extremely sensitive detection of Tb(III) chelates and also of biologically interesting compounds if these chelates are used as labels in bioaffinity assays. The suitability of silicon electrodes coated with thermally grown silicon dioxide film as disposable working electrodes in sensitive time-resolved ECL measurements is demonstrated, and a rapid electrochemiluminoimmunoassay (ECLIA) of human C-reactive protein (hCRP) is described. Tb(III) chelate labels can be detected almost down to picomolar level, and the calibration curve of these labels covers more than 6 orders of magnitude of chelate concentration. The calibration curve of the present immunometric hCRP assay was found to be linear over a wide range, ∼4 orders of magnitude of hCRP concentration, the detection limit of the protein being 0.3 ng mL^{-1} (mean background + 2SD) on CV values of about 10−30%, depending on the immunoassay incubation time. In the ECLIA measurements, different incubation times were tested from 15 min (giving above-mentioned performance) to as short as only 2 min, which still gave successful results with ∼20 000 times better detection limit levels than traditional commercial assay methods. During the ECLIA process, also the Si electrode surface morphology was also investigated by atomic force microscope monitoring.

There is coercive evidence that C-reactive protein (CRP) is a sensitive marker for the development of cardiovascular disease in the general population, and recent studies suggest that CRP is not only a biomarker but also an active crucial mediator in the pathogenesis of atherosclerosis.[1−8] CRP can provide prognostic information about risk of future coronary events in apparently healthy persons. This application requires higher sensitivity assays than have been available in clinical laboratories. Traditional assay methods for CRP have lacked the ability to measure CRP levels below 8000 ng mL^{-1} with sufficient accuracy.[1,2]

CRP is a pentameric acute-phase reactant that is synthesized by the liver. Its production is controlled primarily by interleukin-6. CRP belongs to the pentraxin family of calcium-dependent ligand-binding plasma proteins. The human CRP (hCRP) molecule (MW 115 135) is composed of five identical nonglycosylated polypeptide subunits (MW 23 027), each containing 206 amino acid residues. The protomers are noncovalently associated in an annular configuration with cyclic pentameric symmetry.[1,9] In healthy young adult volunteer blood donors, the median concentration of CRP is reported to be 800 ng mL^{-1} (90% of samples containing less than 3000 ng mL^{-1} and 99% less than 10 000 ng mL^{-1})[10] but following an acute-phase stimulus, values may increase from less than 50 ng mL^{-1} to more than 500 000 ng mL^{-1}. Plasma CRP is produced only by hepatocytes, predominantly under transcriptional control by the cytokine interleukin-6. This hepatic synthesis starts very rapidly after a single stimulus, serum concentration rising above 5000 ng mL^{-1} in ∼6 h and peaking in ∼48 h. The plasma half-life of CRP is ∼19 h and is constant under all conditions of health and disease, so that the only determinant of circulating CRP concentration is the synthesis rate,[11] which thus directly reflects the intensity of the pathological process or processes stimulating CRP production. When the stimulus for increased production completely ceases, the circulating CRP concentration falls rapidly, at almost the rate of plasma CRP clearance. Thus, CRP levels can keep changing in a large tolerance in a short period of time. Also, this very fast response of CRP

* Corresponding author. Tel.: +358-2-3336716. Fax: +358-2-3336700. E-mail: timo.ala-kleme@utu.fi.

† University of Turku.

‡ Helsinki University of Technology.

§ Åbo Akademi University.

(1) Pepys, M. B.; Hirschfield, G. M. *J. Clin. Invest.* **2003**, *111*, 1805−1812.
(2) Labarrere, C. A.; Zaloga, G. P. *Am. J. Med.* **2004**, *117*, 499−507.
(3) van der Meer, I. M.; de Maat, M. P. M.; Hak, A. E.; Kiliaan, A. J.; Del Sol, A. I.; van derKuip, D. A. M.; Nijhuis, R. L. G.; Hofman, A.; Witteman, J. C. M. *Stroke* **2002**, *33*, 2750−2755.
(4) Koenig, W.; Sund, M.; Frohlich, M.; Fischer, H. G.; Lowel, H.; Doring, A.; Hutchinson, W. L.; Pepys, M. B. *Circulation* **1999**, *99*, 237−242.
(5) Ridker, P. M.; Buring, J. E.; Shih, J.; Matias, M.; Hennekens, C. H. *Circulation* **1998**, *98*, 731−733.
(6) Du Clos, T. W. *Sci. Med.* **2002**, *8*, 108−117.
(7) Benzaquen, L. R.; Yu, H.; Rifai, N. *Crit. Rev. Clin. Lab. Sci.* **2002**, *39*, 459−497.
(8) De Ferranti, S.; Rifai, N. *Clin. Chim. Acta* **2002**, *317*, 1−15.
(9) Thomson, D.; Pepys, M. B.; Wood, S. P. *Structure* **1999**, *7*, 169−177.
(10) Shine, B.; de Beer, F. C.; Pepys, M. B. *Clin. Chim. Acta* **1981**, *117*, 13−23.
(11) Vigushin, D. M.; Pepys, M. B.; Hawkins, P. N. *J. Clin. Invest.* **1993**, *91*, 1351−1357.

10.1021/ac051157i CCC: $33.50
Published on Web 11/25/2005

makes it an interesting analyte and adds to the requirement to measure CRP levels in the high-sensitivity levels of 300−10∼000 ng mL^{-1} for the needs of future technology for identifying patients at average (1000−3000 ng mL^{-1}) or high (over 3000 ng mL^{-1}) risk of cardiovascular disease, even among those without a previous history of cardiovascular disease.[1,2,12−16]

In addition to predicting recurrent cardiovascular events in patients with atherosclerotic disease, elevated levels of CRP are reported to be one of the strongest predictors of progressive vascular disease [1−8] and also future cardiovascular events in seemingly healthy people.[1,2,4,5,17−19] Immunoassays for CRP with greater sensitivity than those previously in routine use have revealed that increased CRP values, even within the range previously considered normal, strongly predict future coronary events. During the acute-phase response to infection, inflammatory disease, surgery, trauma, and cancer concentrations of CRP in blood increase by many orders of magnitude and return to normal levels under 1000 ng mL^{-1} with resolution of the disease.[1,2] In contrast with acute inflammation, CRP levels are minimally elevated beneath 10 000 ng mL^{-1} in patients at risk of atherosclerotic disease and they remain elevated for many months up to years. Based on the research material, elevated levels also predict recurrent ischemia and death among those with known atherosclerotic disease, such as stable and unstable angina, those undergoing percutaneous angioplasty, and those who present with the acute coronary syndrome or myocardial infarction.[20−28] In the acute coronary syndrome, elevated levels predict recurrent myocardial infarction independent of troponin levels, suggesting that CRP is not just a marker for myocardial damage.[27,28] Concentration levels also seem to predict recurrent events in patients with stroke[29,30] and may be a marker for restenosis following percutaneous coronary intervention.[31,32]

These new findings and the fact that the traditional CRP determination methods in the clinical laboratory lack the desired sensitivity with the needs of future development toward the point-of-care testing (POCT) together triggered a widespread interest to develop commercial CRP determination methods with high sensitivity.[33−39] Recently, Miao and Bard reported in this journal a high-sensitivity sandwich-type immunoassay for CRP utilizing Au plates or polystyrene microspheres/beads as the supporting heterogeneous phase of the assay and derivatives of tris(2,2′-bipyridyl)ruthenium(II) ($Ru(bpy)_3^{2+}$) as electrochemiluminescent labels.[40−42] In this detection method based on anodic electrochemiluminescence (ECL), they used organic solvent containing tripropylamine as coreactant in the measuring buffer solution. They reported the detection limit to be 10 ng mL^{-1} and found the ECL intensity to be proportional to the analyte CRP concentration over the range of 10.0−10 000 ng mL^{-1}.[42] These capacity levels are lower than those obtained with most of the presently available automated high-sensitivity CRP assay systems.[24]

In this paper, we report a simple (even sufficiently simple for POCT applications) and rapid high-sensitivity heterogeneous electrochemiluminoimmunoassay (ECLIA) method of hCRP based on cathodic hot-electron-induced ECL and time-resolved detection of a Tb(III) chelate label in fully aqueous solution. As we have previously demonstrated, the present novel hot-electron-induced cathodic ECL is based on the use of thin insulating film-coated cathodes, such as, oxide-coated silicon (or aluminum) electrodes, and pulsed electrical excitation of electrochemiluminescent labels. This enables extremely sensitive detection of analytes especially on the basis of time-resolved (TR)-ECL measurements and the use of labels displaying long-lived ECL, such as rare earth chelates, most preferably Tb(III) chelates.[43−47] Although hot-electron-induced cathodic ECL also allows the efficient use of some of the

(12) Ridker, P. M.; Cushman, M.; Stampfer, M. J.; Tracy, R. P.; Hennekens, C. H. *N. Engl. J. Med.* **1997**, *336*, 973−979.
(13) Ridker, P. M.; Rifai, N.; Rose, L.; Buring, J. E.; Cook, N. R. *N. Engl. J. Med.* **2002**, *347*, 1557−1565.
(14) Albert, C. M.; Ma, J.; Rifai, N.; Stampfer, M. J.; Ridker, P. M. *Circulation* **2002**, *105*, 2595−2599.
(15) Ridker, P. M.; Rifai, N.; Clearfield, M.; Downs, J. R.; Weis, S. E.; Miles, J. S.; Gotto, A. M. Jr. *N. Engl. J. Med.* **2001**, *344*, 1959−1965.
(16) Harris, T. B.; Ferrucci, L.; Tracy, R. P.; Corti, M. C.; Wacholder, S.; Ettinger, W. H. Jr.; Heimovitz, H.; Cohen, H. J.; Wallace, R. *Am. J. Med.* **1999**, *106*, 506−512.
(17) Rifai, N. *Card. Toxicol.* **2001**, *1*, 153−157.
(18) Rifai, N.; Ridker, P. M. *Clin. Chem.* **2001**, *47*, 403−411.
(19) Rifai, N.; Ridker, P. M. *Clin. Chem.* **2001**, *47*, 28−30.
(20) Haverkate, F.; Thompson, S. G.; Pyke, S. D.; Gallimore, J. R.; Pepys, M. B. *Lancet* **1997**, *349*, 462−466.
(21) Ridker, P. M.; Rifai, N.; Pfeffer, M. A.; Sacks, F. M.; Moye, L. A.; Goldman, S.; Flaker, G. C.; Braunwald, E. *Circulation* **1998**, *98*, 839−844.
(22) Ferreiros, E. R.; Boissonnet, C. P.; Pizarro, R.; Merletti, P. F.; Corrado, G.; Cagide, A.; Bazzino, O. O. *Circulation* **1999**, *100*, 1958−1963.
(23) Lindahl, B.; Toss, H.; Siegbahn, A.; Venge, P.; Wallentin, L. *N. Engl. J. Med.* **2000**, *343*, 1139−1147.
(24) Roberts, W. L.; Moulton, L., Law, T. C.; Farrow, G.; Cooper-Andersson, M.; Savory, J.; Rifai, N. *Clin. Chem.* **2001**, *47*, 418−425.
(25) Milazzo, D.; Biasucci, L. M.; Luciani, N.; Martinelli, L.; Canosa, C.; Schiavello, R.; Maseri, A.; Possati, G. *Am. J. Cardiol.* **1999**, *84*, 459−461.
(26) Zebrack, J. S.; Muhlestein, J. B.; Horne, B. D.; Anderson, J. L. *J. Am. Coll. Cardiol.* **2002**, *39*, 632−637.
(27) Benamer, H.; Steg, P. G.; Benessiano, J.; Vicaut, E.; Gaultier, C. J.; Boccara, A.; Aubry, P.; Nicaise, P.; Brochet, E.; Juliard, J. M.; Himbert, D.; Assayag, P. *Am. J. Cardiol.* **1998**, *82*, 845−850.
(28) Rebuzzi, A. G.; Quaranta, G.; Liuzzo, G.; Caligiuri, G.; Lanza, G. A.; Gallimore, J. R.; Grillo, R. L.; Cianflone, D.; Biasucci, L. M.; Maseri, A. *Am. J. Cardiol.* **1998**, *82*, 715−719.
(29) Di Napoli, M.; Papa, F.; Bocola, V. *Stroke* **2001**, *32*, 917−924.
(30) Di Napoli, M.; Papa, F.; Bocola, V. *Stroke* **2001**, *32*, 133−138.
(31) Walter, D. H.; Fichtlscherer, S.; Britten, M. B.; Rosin, P.; Auch-Schwelk, W.; Schachinger, V.; Zeiher, A. M. *J. Am. Coll. Cardiol.* **2001**, *38*, 2006−2012.
(32) Chew, D. P.; Bhatt, D. L.; Robbins, M. A.; Penn, M. S.; Schneider, J. P.; Lauer, M. S.; Topol, E. J.; Ellis, S. G. *Circulation* **2001**, *104*, 992−997.
(33) Koskinen, J. O.; Vaarno, J.; Meltola, N. J.; Soini; J. T.; Hänninen, P. E.; Luotola, J.; Waris, M. E.; Soini, A. E. *Anal. Biochem.* **2004**, *328*, 210−218.
(34) Nilsson, S.; Lager, C.; Laurell, T.; Birnbaum, S. *Anal. Chem.* **1995**, *67*, 3051−3056.
(35) Holownia, P.; Perez-Amodio, S.; Price, C. P. *Anal. Chem.* **2001** *73*, 3426−3431.
(36) Perez-Amodio, S.; Holownia, P.; Davey, C. L.; Price, C. P. *Anal. Chem.* **2001**, *73*, 3417−3425.
(37) Park, J.; Kurosawa, S.; Watanabe, J.; Ishihara, K. *Anal. Chem.* **2004**, *76*, 2649−2655.
(38) Liron, Z.; Bromberg, A.; Fisher, M., Eds. *Novel Approaches in Biosensors and Rapid Diagnostic Assays*; Kluwer Academic/Plenum Publishers: New York, 2000.
(39) Christodoulides, N.; Tran, M.; Floriano, P. N.; Rodriquez, M.; Goodey, A.; Ali, M.; Neikirk, D.; McDevitt, J. T. *Anal. Chem.* **2002**, *74*, 3030−3036.
(40) Miao, W.; Bard, A. J. *Anal. Chem.* **2003**, *75*, 5825−5834.
(41) Miao, W.; Bard, A. J. *Anal. Chem.* **2004**, *76*, 5379−5386.
(42) Miao, W.; Bard, A. J. *Anal. Chem.* **2004**, *76*, 7109−7113.
(43) Kulmala, S.; Suomi, J. *Anal. Chim. Acta.* **2003**, *500*, 21−69.
(44) Kulmala, S.; Ala-Kleme, T.; Latva, M.; Loikas, K.; Takalo, H. *J. Fluoresc.* **1998**, *8*, 59−65.
(45) Helin, M.; Väre, L.; Håkansson, M.; Canty, P.; Hedman, H.-P.; Heikkilä, L.; Ala-Kleme, T.; Kankare, J.; Kulmala, S. *J. Elecroanal. Chem.* **2002**, *524−525*, 176−183.
(46) Eskola, J. U.; Mäkinen, P.; Oksa, L.; Loikas, K.; Nauma, M.; Håkansson, M.; Kulmala, S. *Anal. Chim. Acta* **2002**, *458*, 271−280.
(47) Ala-Kleme, T.; Kulmala, S.; Latva, M. *Acta Chem. Scand.* **1997**, *51*, 541−546.

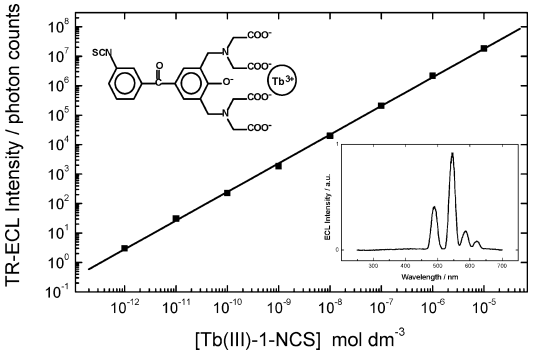

Figure 1. Structure of the Tb(III)-1-NCS chelate and dependence of the TR-ECL intensity on the Tb(III)-1-NCS chelate concentration at oxide-covered Si electrodes. The calibration curve was measured with a Perkin-Elmer Wallac electroluminometer in the ECLIA measuring buffer (0.2 M boric acid, pH 7.8, containing 0.1% NaN_3) The spectrum of the Tb(III)-1-NCS chelate in the inset was measured with a Perkin-Elmer LS-5 spectroluminometer with the excitation slit closed and emission slit 20 nm, gate time 13 ms, scanning speed 240 nm min^{-1}, and equipped with a microprosessor-controlled coulostatic pulse generator adjusted to yield 120 μC cathodic pulses with −40 V applied pulse voltage with 80 Hz frequency.

best known electrochemiluminescent labels, such as derivatives of luminol and $Ru(bpy)_3^{2+}$ [48,49] normally used in the better established anodic ECL applications, Tb(III) chelate labels are the best labels for our method providing the highest sensitivity. These labels offer an overall increase in detection ability and considerably improve the S/N ratio due to the relatively long-lived luminescence of the label and short-lived background emission with TR-ECL detection. The benefits of this new technology for various bioaffinity assay types, and especially for POCT analysis, are also pointed out.

EXPERIMENTAL SECTION

Chemicals and Materials. The monoclonal anti-hCRP primary and secondary antibodies (monoclonal Anti-hCRP clone 6405 1.00 mg mL^{-1} and clone 6404 2.22 mg mL^{-1}, respectively) were purchased from Medix Biochemica Oy (Ab, Finland). The hCRP standard solution (3,23 mg mL^{-1}) was obtained from Scripps Laboratories (San Diego, CA). Sodium tetraborate decahydrate, sodium azide, Tween 20, Na_2CO_3, $NaH_2PO_4 \cdot H_2O$, $Na_2HPO_4 \cdot 12H_2O$, hydrofluoric acid, H_2SO_4, and HCl were purchased from Merck. Tris, bovine γ-globulin, and bovine serum albumin (BSA) were products of Aldrich. $CaCl_2 \cdot 6H_2O$, NaCl, D-sorbitol, and 1-propanol were obtained from Riedel-de Haën, Oy FF-Chemicals Ab, ICN Biomedicals Inc., and LabScan, respectively. The following reagents need precautions: azide ion is toxic and forms explosive salts with heavy metal ions, HF is corrosive and very toxic. The isothiocyanate derivative of Tb(III)-1 chelate (Tb(III)-1-NCS) (1 = 2,6-bis[*N*,*N*-bis(carboxymethyl)aminomethyl]-4-benzoylphenol) (Figure 1) was synthesized as described previously.[50] Silicon wafers 100.0-mm-diameter boron doped p-type (100) 0.525 mm thick with resistivities of 10.0−20.0 mΩ·cm were purchased from Okmetic Oyj. Quartz-distilled water was used for the preparation of all solutions.

Manufacturing of the Labeling Antibody. Tb(III)-1-NCS chelate was used as a labeling molecule for the secondary anti-hCRP antibody. The formation of the Tb(III)-1-Ab-hCRP-label was based on the well-known reaction between the isothiocyanate group of the Tb(III)-1 chelate and the amino groups of the secondary anti-hCRP antibody. The labeling reaction was carried out overnight at room temperature with a 70-fold molar excess of the chelate in 0.5 M Na_2CO_3 at pH 9.0. Excess label was removed by gel filtration on a NAP-10 column (containing Sephadex G-25, Pharmacia) with Tris−saline−azide (TSA) buffer (50 mM Tris, 0.9% NaCl, 0.05% NaN_3, pH 7.7, adjusted with HCl). The needed buffer exchanges were made with the help of an NAP-5 column (containing Sephadex G-25, Pharmacia). At the beginning of the labeling antibody preparation PSB buffer consisting of 0.276 g L^{-1} $NaH_2PO_4 \cdot H_2O$, 2.865 g L^{-1} $Na_2HPO_4 \cdot 12H_2O$, and 8.10 g L^{-1} NaCl, pH 7.0, was used for balancing of the NAP-5 column and the change of secondary anti-hCRP antibody buffer solution.

Manufacturing of the Si Electrodes. Si electrodes were made by cutting the silicon wafers into pieces. The insulating oxide films on the cut Si electrode pieces were fabricated by a simplified thermal oxidation process. Briefly, first the Si electrodes were washed 5 min in 1-propanol and then soaked for 10 s in the 5% HF solution, after which they were carefully rinsed in the running quartz distilled water. Thermal oxides were then grown in a Vulcan 3-550 oven (NEY Dental International) at 800 °C for 10 min, producing an oxide film thickness of ~4 nm. For practical reasons, the washing and thermal oxidation processes were performed using a batch method for large amounts of electrodes at a time. The thicknesses of the oxide films were spot checked with a Gaertner L 116 S ellipsometer by using the 632.8-nm wavelength (He−Ne laser), measuring angle 70° and polarization angle 45° as described earlier.[51]

Coating and Saturation of the Si Electrodes. In the heterogeneous immunometric hCRP assay, oxide-covered Si electrodes (size 20 × 4.0 mm) were coated with monoclonal anti-hCRP primary antibodies by physical adsorption by incubating the electrodes in coating solution. The coating was performed batchwise, immersing Si electrodes in microtiter strips containing 250 μL of coating solution consisting of 5 μg mL^{-1} primary anti-hCRP in TSA buffer (50 mM Tris, 0.9% NaCl, 0.05% NaN_3, pH 7.7, adjusted with HCl). The coated area was 10 × 4.0 mm in both sides of the Si electrodes. The reaction was incubated overnight at room temperature in a humid plastic container. Next, the coated Si electrodes were moved to the other microtiter strips containing 350 μL of the saturation solution (50 mM Tris, 6.0% D-sorbitol, 1 mM $CaCl_2 \cdot 6H_2O$, 0.1% BSA, pH 7.7, adjusted with HCl) and allowed to stand overnight in a humid plastic container as before. The purpose of this saturation procedure was to prevent the nonspecific absorption of the secondary label antibody. Coated and saturated Si plate electrodes were kept ready for the assays in plastic container at +4 °C.

(48) Kulmala, S.; Ala-Kleme, T.; Kulmala, A.; Papkovsky, D.; Loikas, K. *Anal. Chem.* **1998**, *70*, 1112−1118.
(49) Ala-Kleme, T.; Kulmala, S.; Väre, L.; Juhala, P.; Helin, M. *Anal. Chem.* **1999**, *71*, 5538−5543.
(50) Kankare, J.; Karppi, A.; Takalo, H. *Anal. Chim. Acta* **1994**, *295*, 27−35.
(51) Helin, M.; Väre, L.; Håkansson, M.; Canty, P.; Hedman, H.-P.; Heikkilä, L.; Ala-Kleme, T.; Kankare, J.; Kulmala, S. *J. Electroanal. Chem.* **2002**, *524−525*, 176−183.

hCRP Immunoassay. The heterogeneous immunoassay at oxide-covered Si electrodes coated with the primary antibodies was carried out by adding a mixture of hCRP calibration standards (100.0 μL) and the Tb(III)-1-Ab-hCRP-label (100.0 μL, the final concentration of the Tb(III)-1-Ab-hCRP-label was 82 ng mL^{-1}) diluted in assay buffer in the microtiter strips. The assay buffer consisted of 50 mM Tris (pH 7.7), 0.9% NaCl, 0.05% NaN_3, 0.5% BSA, 1.0 mM $CaCl_2 \cdot 6H_2O$, 0.05% bovine γ-globulin, and 0.01% Tween 20. Different incubation times were tested and typically incubation times used were between 2 and 15 min. After the incubation, the Si electrodes were washed three times in microtiter wells with 300 μL of the washing solution containing 9 g L^{-1} NaCl, 1 g L^{-1}, NaN_3, and 0.2 g L^{-1} Tween 20 by agitating in the shaker for 2 min. The washing process was important for preventing the nonspecific binding and for achieving the best possible signal-to-background ratio. Another purpose for this washing procedure was to stop the incubation reaction at exactly same time for all Si electrodes. The ECLIA measurements with the Si electrodes were carried out in 0.2 M boric acid measuring buffer (pH 7.8 adjusted with H_2SO_4) containing 0.1% NaN_3 in the microtiter strips modified cell, described detailed elsewhere.[52] In the ECLIA measurements, the volume of the measuring buffer in the microtiter strips was 250 μL. The TR-ECLIA measurements were carried out with a semiautomatic electroluminometer modified from a Perkin-Elmer Wallac electrofluorometer. The electroluminometer was equipped with an internal potentiostatic pulse generator, and the used pulse voltage, length, and frequency were −10 V, 200 μs, and 200 Hz, respectively. The measurements were made using TR detection mode, in which the delay after the end of the electrical excitation pulse was 90 μs and the width of the detection window was 1.50 ms. The general principle of the used heterogeneous immunometric sandwich-type immunoassay of hCRP analyte is shown in Figure S1 (Supporting Information).

Other Instrumentation. Differently from all the ECLIA and the Tb(III)-1-NCS chelate ECL calibration curve measurements, the spectra of Tb(III)-1-NCS chelate (inset in Figure 1) was recorded with a Perkin-Elmer LS-5 spectroluminometer excitation shutter closed equipped with a microprosessor-controlled coulostatic pulse generator. The sample cell consisted of a 1-cm spectrophotometer quartz cuvette, a Teflon sample holder, and Si/SiO_2 plate and Pt wire electrodes. The sample holder has a window that restricted the working electrode surface area to 1.1 cm^2, and the cell volume was 1.0 mL. The atomic force microscopy (AFM) measurements were made with a Nanoscope IIIa instrument operated in the tapping mode (Digital Instruments Inc., Santa Barbara, CA). The absorbance measurements presented in the Supporting Information were carried out on a Hewlett-Packard 8453 UV−visible spectrophotometer.

RESULTS AND DISCUSSION

Basic Features of Tb(III) Chelate ECL. Currently, aromatic lanthanide chelates, mainly phenolic Tb(III) chelates, are the best labels known to be used in our type of ECLIA.[44,53−56] Contrary to the other luminescent lanthanide ions, Tb(III) is very redox inert[57] and has its resonance energy in a nice level for the energy transfer to occur from the triplet states of various aromatic compounds.[57,58] Furthermore, the luminescence lifetime of the Tb(III) ion that is well-screened from water molecules by a multidentate ligand is of the order of 1.7−2.4 ms; in the case of this Tb(III)-1-NCS chelate used in this work, it was measured to be 2.1 ms. Due to this long-lived luminescence, it is possible to use efficiently TR measuring techniques and achieve excellent signal-to-noise ratio.[55,59−61] Thus, TR-ECL measurements provide the same sensitivity of detection as the time-resolved photoluminescence of lanthanide(III) chelates, but the benefits of ECL appear mainly in development of small-sized, low-cost devices for POCT or, for example, doctor's office use due to the simple electronics and overall construction.

According to previous studies,[48,49,62,63] this kind of higher technical simplicity for certain applications is based on the use of cathodically pulse-polarized, disposable, thin insulating film-coated working electrodes such as oxide-coated silicon electrodes combined with a quite freely selectable counter electrode. The presently used thermal oxidation is probably the simplest method to form an amorphous, insulating SiO_2 film over a silicon substrate. Thermally grown SiO_2 is known to be an excellent insulator, and the Si/SiO_2 interface formed by thermal oxidation is also known to have very low number of interface states.[64,65] This is the main reason for using thermally oxidized silicon in electrical applications where the high-purity oxide and high-quality interface are required, and this is also the reason thermally grown SiO_2 is perfect for our purposes.

As the primary step, the cathodic pulse polarization of thin oxide film-coated silicon electrodes induces a tunnel emission of hot electrons (e_{hot}^-) into aqueous electrolyte solutions. This results in a subsequent generation of hydrated electrons (e_{aq}^-) and oxidizing radicals such as sulfate and hydroxyl radicals from added coreactants or dissolved oxygen.[44,48,62,63] As is known, e_{hot}^- and e_{aq}^- can react with compounds very difficult to reduce, and therefore, cathodic reductions usually not possible to carry out in aqueous solutions can be made.[62] In addition to reduction of labels, there is still plenty of e_{hot}^- and e_{aq}^- available to react with added coreactants such as peroxodisulfate, hydrogen peroxide, or dissolved oxygen, which form highly oxidizing sulfate or hydroxyl radicals upon one-electron reduction nearly at diffusion-controlled rates. In the present case, when special added coreactants are not used, the oxidizing hydroxyl radicals (•OH) are mainly formed from molecular oxygen in aqueous electrolyte

(52) Håkansson, M.; Jiang, Q.; Suomi, J.; Loikas, K.; Nauma, M.; Ala-Kleme, T.; Kankare, J.; Juhala, P.; Eskola, J.; Kulmala, S., Cathodic electrochemiluminescence at double barrier $Al/Al_2O_3/Al/Al_2O_3$ tunnel emission electrodes. *Anal. Chim. Acta*, in press.

(53) Richter, M.; Bard A. *Anal. Chem.* **1996**, *68*, 2641−2650.

(54) Ala-Kleme T.; Haapakka, K.; Latva, M. *J. Alloys Compd.* **1998**, *275−277*, 911−914.

(55) Ala-Kleme, T.; K. Haapakka, M. Latva *Anal. Chim. Acta* **2000**, *403*, 161−171.

(56) Kulmala, S.; Helin, M.; Ala-Kleme, T.; Väre, L.; Papkovsky, D.; Korpela, T.; Kulmala, A. *Anal. Chim. Acta* **1999**, *386*, 1−6.

(57) Carnall, W. In *Handbook on the Physics and Chemistry of Rare Earths*; Gschneider, K. Jr., Eyring, L., Eds.; North-Holland: Amsterdam, 1979; Vol. 3, pp 171−208.

(58) Reisfeld, R. *J. Res. Natl. Bur. Stand. U.S. Sect. A* **1972**, *76*, 613−635.

(59) Kankare, J.; Fälden, K.; Kulmala, S.; Haapakka, K. *Anal. Chim. Acta* **1992**, *256*, 17−28.

(60) Kulmala, S.; Haapakka, K. *J. Alloys Compd.* **1995**, *225*, 502−506.

(61) Kulmala, S.; Kulmala, A.; Ala-Kleme, T.; Pihlaja, J. *Anal. Chim. Acta* **1998**, *367*, 17−31.

(62) Kulmala, S.; Ala-Kleme, T.; Heikkilä, L.; Väre, L. *J. Chem. Soc., Faraday Trans.* **1997**, *93*, 3107−3113.

(63) Ala-Kleme, T.; Kulmala, S.; Latva, M. *Acta Chem. Scand.* **1997**, *57*, 541−546.

(64) Barron, A. R. *Adv. Mater. Opt. Electron.* **1996**, *6*, 101−114.

(65) Frosh, C. J.; Derick, L. *J. Electrochem. Soc.* **1957**, *104*, 547−552.

solutions according to reactions 1−3 (second-order rate constants for reactions 1−3 are $k_1 = 1.9 \times 10^{10}$ L moL^{-1} s^{-1}, $k_2 = 1.3 \times 10^{10}$ L moL^{-1} s^{-1}, $k_3 = 1.2 \times 10^{10}$ L moL^{-1} s^{-1}, respectively).[66]

$$O_2 + e_{aq}^- \rightarrow O_2^{\bullet -} \quad (1)$$

$$O_2^{\bullet -} + e_{aq}^- + 2H_2O \rightarrow H_2O_2 + 2OH^- \quad (2)$$

$$H_2O_2 + e_{aq}^- \rightarrow OH^- + {}^{\bullet}OH \quad (3)$$

On the other hand, azide ion (N_3^-), which is present in the used measuring buffer and is demonstrated to be very useful as an ECL enhancer due to decreasing effect of background signal,[61] reacts near diffusion-controlled rate with hydroxyl radical producing azide radical (reaction 4, second-order rate constant $k_4 = 1.2 \times 10^{10}$ L moL^{-1} s^{-1}).[66]

$$^{\bullet}OH + N_3^- \rightarrow OH^- + N_3^{\bullet} \quad (4)$$

As has been presented earlier,[63] another parallel reaction pathway for generation of hydroxyl radical is that E'_1 centers, i.e., one electron trapped in an anion vacancy of SiO_2, and the empty anion vacancies can act as strongly oxidizing species having an oxidizing power between the hydroxyl radical and sulfate radical at pH 8. So these surface species can oxidize hydroxide ions and surface hydroxyl groups of the oxide to hydroxyl radicals, which can act as oxidizing mediators in the absence of purposely added core-actants. Briefly, the strong reductant in our system is considered to be e_{hot}^- or e_{aq}^- generated during the cathodic pulse polarization of the Si electrode by direct tunnel emission of electrons into the aqueous electrolyte solution.[62,63,67] The strong oxidant is the hydroxyl radical formed at nearly diffusion-controlled rate via three-step reduction of molecular oxygen (reactions 1−3) if hydrated electrons are present[66] or most likely hydroxyl radicals formed with the reaction of E'_1 centers and the empty anion vacancies.[63] Hence, highly reducing and oxidizing conditions are simultaneously achieved in the vicinity of the electrode surface, and one of the harshest conditions in aqueous solutions that can exist is formed, capable of generating chemiluminescence from a wide variety of compounds that otherwise are hard to reduce or hard to oxidize.

Aromatic Tb(III) chelates show chemiluminescence based on either ligand−reduction−initiated oxidative excitation pathway (Red−Ox pathway) or on ligand−oxidation−initiated reductive excitation pathway (Ox−Red pathway), which involve one-electron reduction/oxidation of ligand to a radical species followed by one-electron oxidation/reduction of the ligand radical. If the oxidant/reductant of the second step is strong enough, the ligand is formed in its original oxidation state but now in its excited state. The ligand transfers its excitation energy intramolecularly to the central Tb^{3+} ion by the photophysical processes well known from the photoluminescence studies of these chelates, and finally, the central Tb^{3+} ion emits light by $^5D_4 \rightarrow {}^7F_J$ transitions shown in the spectra inset of Figure 1. In the particular case of Tb(III)-1-NCS chelate shown in this paper, the predominant reaction pathway is the latter mentioned Ox−Red pathway using hydroxyl radical as a strong oxidant (reactions 5−9) based on detailed earlier studies.[44,48,61]

$$\text{Tb(III)-1-NCS} + {}^{\bullet}OH \rightarrow \text{Tb(III)-1}_{Ox}\text{-NCS} + OH^- \quad (5)$$

$$\text{Tb(III)-1}_{Ox}\text{-NCS} + e_{aq}^- \rightarrow \text{Tb(III)-}^1\text{1*-NCS} \quad (6)$$

$$\text{Tb(III)-}^1\text{1*-NCS} \rightarrow \text{Tb(III)-}^3\text{1*-NCS} \quad (7)$$

$$\text{Tb(III)-}^3\text{1*-NCS} \rightarrow {}^*\text{Tb(III)-1-NCS} \quad (8)$$

$$^*\text{Tb(III)-1-NCS} \rightarrow \text{Tb(III)-1-NCS} + h\nu_J \quad (9)$$

Analysis of the Label. The prepared Tb(III)-1-Ab-hCRP label was tested with two independent methods. Figure 1 presents the dependence of the ECL intensity on the concentrations of Tb(III)-1-NCS chelate (the structure of the chelate is shown as the inset in Figure 1). As shown in the figure, the chelate can be detected almost even down to picomolar level and the calibration curve of the chelate covers more than 6 orders of magnitude of chelate concentration as measured with TR-ECL detection method. The corresponding TR-ECL intensity of the Tb(III)-1-Ab-hCRP-label is shown in the Supporting Information, Figure S2. First the concentration of the Tb(III)-1-NCS chelate in the Tb(III)-1-Ab-hCRP-label was calculated by comparing the calibration curves of the chelate (ECL intensity $0.97c + 12.1$) and the label [log-(ECL of concentrated Tb(III)-1-Ab-hCRP-label) 8,27] (Figure S2). According to these results, the preparation of the Tb(III)-1-Ab-hCRP-label was successful and the concentration of chelate was calculated to be $\sim 1.13 \times 10^{-4}$ M in the concentrated Tb(III)-1-Ab-hCRP-label solution. Another method to detect the chelate concentration in the label was based on absorption measurements of the Tb(III)-1-NCS chelate, anti-hCRP secondary antibody, and Tb(III)-1-Ab-hCRP-label (Figure S3). According to the absorbance results (Table S1), the calculated concentration of the isothiocyanate derivative of Tb(III)-1 chelate was 1.01×10^{-4} M in the concentrated Tb(III)-1-Ab-hCRP-label solution (Supporting Information). The mean value of the chelate concentration in the label was then $\sim 1.1 \times 10^{-4}$ M. Thus, based on both of these above-mentioned measurements, the labeling degree of the antibody was determined to be ~18 Tb(III)-1 chelate/antibody molecule (detailed calculations in the Supporting Information).

AFM-Monitored Surface Morphology of Si Electrode During the ECLIA. The rms roughness values calculated from measured 1×1 μm^2 image areas (Figure 2) were noticed to describe clearly the surface morphology of Si electrodes monitored on different stages of the ECLIA process by AFM. The rms roughness of natural oxide layer of the crude silicon wafers, which was approximated to be ~1 nm thick according to the ellipsometer measurements, was 0.26 nm with height scale of 3 nm and height of globular objects 1−4 nm (Figure 2a). In the next step (Figure 2b) where the Si electrodes were covered with 4-nm-thick oxide films, the optimum thickness on behalf of ECL, the rms roughness was 0.32 nm with height scale of 5 nm and height of globular objects 1−4 nm. So the calculated rms roughness factor was increased a little bit, as could be expected when the oxide layer was grown thicker by thermal oxidation. The rms roughness was

(66) Buxton, G.; Greenstock, C.; Helman, W.; Ross, A. *J. Phys. Chem. Ref. Data* **1988**, *17*, 1027−1284.
(67) Kulmala, S.; Ala-Kleme, T.; Joela, H.; Kulmala, A. *J. Radioanal. Nucl. Chem.* **1998**, *232*, 91−95.

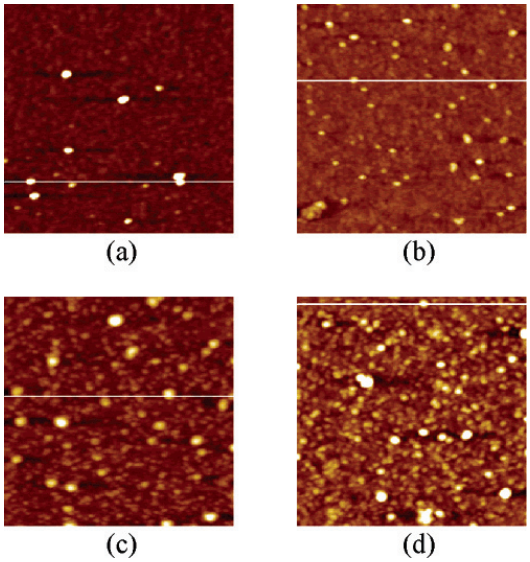

Figure 2. Surface structure of a silicon electrode in different stages of the ECLIA process as monitored by AFM. Conditions: all image sizes 1 × 1 μm^2, (a) natural oxide film on the Si electrode measured after cutting silicon wafers into the pieces without any other treatment, (b) Si electrode covered with ~4-nm-thick thermal oxide film, (c) Si electrode coated with primary anti-hCRP antibodies, and (d) coated and saturated Si electrode.

still increased after the monitored surface of the Si electrode was coated with anti-hCRP primary antibodies (Figure 2c), being 1.06 nm with height scale of 10 nm and height of globular objects 1−4 (lower) or 6−10 nm (higher). The explanation for this effect is quite simple. Because the coating is based on physical adsorption of the antibodies, it is obvious that these Y-shaped IgG antibodies can be laying, standing up, or between these two orientations. When the IgG molecules are laying, the thickness of the film that they form should be about the value of the smaller dimension of the molecule, which is ~4 nm. The observed results also coincide with the highest thickness of 10 nm, which is equal to the largest dimension of the IgG molecules, i.e., antibodies standing up.[68] All the antibody film thicknesses between 4 and 10 nm are then naturally formed of antibodies fallen down by different degrees. The film thicknesses below the smallest dimension of the IgG molecules could be caused by holes in the antibody film, which is typical for coatings based on physical absorption. This theory is also supported by the observation that after saturation the rms roughness factor of the Si electrodes was decreased to 0.71 nm with height scale of 5 nm and height of globular objects 3−6 nm (Figure 2d). Obviously, due to the saturation process, the holes of the coating film were filled and the surface became smoother compared to the pure coated Si electrode surface.

TR-ECLIA of hCRP and Analytical Application of the Method. Traditionally, most quantitative immunometric measurements have been carried out by incubating the immunoassay reactions to equilibrium or very near to it, in order to gain

(68) Tronin, A.; Dubrovsky, T.; De Nitti, C.; Gussoni, A.; Erokhin, V.; Nicolini C. *Thin. Solid Films* **1994**, *238*, 127−132.

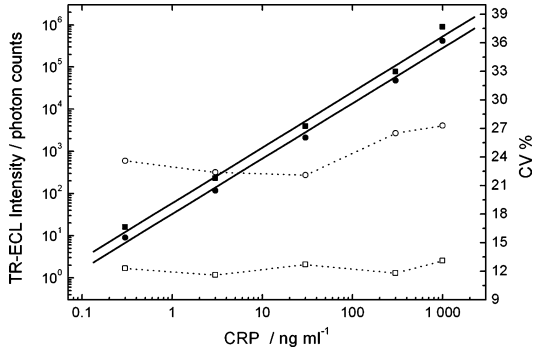

Figure 3. Calibration curve of the immunometric assay of hCRP with incubation times of 15 (■) and 2 (●) min and the corresponding precision profiles presented with dotted lines with incubation times of 15 (□) and 2 (○) min. For details, see the Experimental Section.

sufficient signal and assay sensitivity. However, using label technology sensitive enough to produce a sufficient signal from fewer analyte molecules facilitates the introduction of a kinetic assay format with considerably shorter incubation times. In the heterogeneous sandwich-type ECLIA, the low detection limits achievable with Tb(III) chelate allowed the binding reaction to be stopped before it reached plateau, at the same time retaining the excellent analytical sensitivity and a low detection limit. Of course, also both the used small volumes and relatively concentrated solutions and small surface areas of the Si electrodes used as the solid support of immunoassays made the diffusion-controlled reaction rates fast. Two different ECLIA measurements of hCRP are shown in Figure 3: one reached plateau in under 15 min and the other was stopped before equilibrium was reached after 2 min of incubation by a washing procedure presented in the Experimental Section. Detailed results of kinetic hCRP assay measurements are going to be published later, but according to preliminary measurements, the equilibrium was achieved with our method after 6−7 min of incubation time. The calibration curve for the heterogeneous sandwich-type immunometric immunoassay of hCRP with thermally oxidized working Si electrodes, including its precision profiles, is presented in Figure 3 with two different incubation times. The detection limit of the assay using 15-min incubation time was ~0.3 ng mL^{-1} (mean background + 2SD) with CV of ~11%, so the assay is ultrasensitive, being well below the need of a high-sensitivity region of 300−10 000 ng mL^{-1}.[24] The linear region of the calibration curve covers almost 4 orders of magnitude (0.3−3000 ng mL^{-1}) of hCRP concentration using commercial standard solutions. The effect of the high-dose Hook phenomenon on ECLIA of hCRP was noted to be affected only after a hCRP concentration of 3000 ng mL^{-1} in the immunoassay where 15-min incubation time was used. Thus, in practical normal use, the whole blood, plasma, or serum samples have to be diluted before immunometric hCRP ECLIA measurements. According to these results, it is obvious that the analytical sensitivity and detection limit of this presented ECLIA fulfills greatly the demands of the POCT applications. In fact, the sensitivity and detection limit of the present ECLIA is so low that there is no need to tune up the system to achieve the best possible performance. This is a good thing, for example, considering the research and develop-

ment for POCT, because it makes it possible to make some compromises at the expense of analytical sensitivity and detection limit. Overall, the great sensitivity of the immunoassay method allows the effective exploitation of structural simplicity and effective excitation mechanism of robust product development for POCT applications. The other calibration plot in Figure 3 presents the ECLIA of hCRP measured using a 2-min incubation time. As can be seen, the ECLIA intensity level results are little lower than those for longer incubation times and the CVs are much poorer probably due to the manually made measurements. Anyway if the rather poor CV is not taken into account, the results are quite good, the detection limit being at same level as it was when sn incubation time of 15 min was used, showing the power of this immunometric hCRP ECLIA determination. In addition, the special advantage of the present excitation method is that various label molecules having different redox and optical properties can be simultaneously excited. Another benefit is that both wavelength and time discrimination can be utilized in the separation of the signals emerging from different labels. Thus, the basis is easily created for two-parameter assays, internal standardization, or even multicomponent analysis: for example, with Tb(III) chelates exhibiting a long-lived luminescence and the other parameter with a short luminescence lifetime component, e.g., $Ru(bpy)_3^{2+}$.[49]

CONCLUSIONS

An ultrasensitive sandwich-type immunometric heterogeneous electrochemiluminoimmunoassay of hCRP was developed based on detection of labels by cathodic pulse polarization of disposable, thin insulating film-coated silicon electrodes. The exceptional sensitivity of ECLIA method was based on the use of an isothiocyanate derivative of Tb(III) chelate as a labeling agent for anti-hCRP antibodies. The excellent S/N ratios were provided by the time-resolved detection method. With the present technique, the hCRP detection limit is as low as 0.3 ng mL^{-1} with the calibration curve spanning over ~4 orders of magnitude of concentration. The demonstrated detection limit of hCRP is well below those obtained from most of the presently available automated high-sensitivity CRP assay systems.[24] This also fulfills the demands of future diagnostic tools for measuring hCRP to identify patients at a probable risk in gaining a cardiovascular disease.[1,2,69] The results also strongly suggest the presented method as being a very promising analytical tool for POCT applications due to the low cost of excitation electronics and simple small-size constructability of portable analyzers.

(69) Roberts, W. L.; Schwarz, E. L.; Ayanian, S.; Rifai, N. *Clin. Chim. Acta* **2001**, *314*, 255−259.

ACKNOWLEDGMENT

The aid of Labmaster Ltd. is gratefully thanked.

SUPPORTING INFORMATION AVAILABLE

A general principle of the heterogeneous immunometric sandwich-type immunoassay of hCRP analyte used in this work (Figure S1). A dependence of the ECL intensity on the dilution ratio of Tb(III)-1-Ab-hCRP-label (Figure S2). The absorbance spectra of Tb(III)-1-NCS, anti-hCRP, and Tb(III)-1-Ab-hCRP-label (Figure S3) and the absorbance readings (Table S1) on which the calculations of Tb(III)-1-NCS chelate concentration in the Tb(III)-1-Ab-hCRP-label and the labeling degree approximation are based. This material is available free of charge via the Internet at http://pubs.acs.org.

Received for review June 29, 2005. Accepted October 24, 2005.

AC051157I